Simulation of dissimilar weld joints of steel P91

J. Sopoušek, R. Foret and V. Jan

Results of computer simulations of long term service exposure for weldments of the CSN 15 128/P91 and SK3STC/P91 steels are presented and compared with corresponding results of phase and composition experiments. The welded material P91 (EU designation: X10CrMoVNb 9–1) represents progressive chromium steel alloyed with molybdenum, vanadium, carbon, and nitrogen. The CSN 15 128 (13CrMoV 2–5) material is low alloy Cr–Mo–V steel. The SK3STC alloy (12CrMo 10–10) represents the consumable electrode material. The stability of the weldment microstructure is investigated at elevated temperatures (500–700°C). The simulation method is based on the Calphad approach complemented with the theory of multicomponent bulk diffusion, local conditions of phase equilibrium, and the assumption that diffusion is the process that controls the rate of phase transformation. Significant phase profiles, concentration profiles, and phase transformation processes in the diffusion affected zone are simulated, investigated, and compared with experimental results. The potentially deleterious carbon depleted region inside each weld joint is discussed. The method described can be used to predict microstructure instability in weld joints. *STWJ/374*

Keywords: low alloy steel, kinetic simulation

Dr Sopoušek is in the Faculty of Science, Department of Theoretical and Physical Chemistry, Masaryk University – Brno, Kotlářská 2, CZ–61137 Brno, Czech Republic (sopousek@chemi.muni.cz). Dr Foret (foret@umi.fme.vutbr.cz) and Mr Jan (jan@pime.fme.vutbr.cz) are in the Department of Materials Science, Faculty of Mechanical Engineering, Brno University of Technology, Technická 2, CZ–61669 Brno, Czech Republic. *Manuscript received 13 December 2002; accepted 11 February 2003.*

INTRODUCTION

A weld joint between dissimilar materials under external stress usually represents a critical point in many technical applications at elevated temperatures. The investigation of the relationships between the element/phase redistributions, the microstructure at various points across the weldments, and local mechanical properties represents a method that is suitable for the evaluation of long term mechanical/microstructure stability of weld joints.[1] For weld joint applications at elevated temperatures, the mechanical properties can be related to chemical concentration and phase transformation processes in the diffusion affected zone.[2,3] Information on the time evolution of both the phase and the element redistributions at a given treatment temperature is therefore very important.

The main factors that influence the stability or instability of the weld joint of steels are, above all, carbide nucleation, phase transformation, rate of diffusion,[4] and carbon depletion.[5] These factors are significantly dependent on temperature. Phase transformations in weld joints of multicomponent alloys have become highly complex owing to the high degree of freedom of the multicomponent system.[6,7] The diffusion fundamentally affects the rate of phase transformations at elevated temperatures[4] and the changes in chemical potentials of the alloy elements are consequently the cause of phase precipitations, growth, phase dissolutions, and/or phase boundary replacement in the weld diffusion zone. In many instances, regions parallel to the initial weld interface are formed in the diffusion affected zone, with different microstructures having different mechanical and corrosion resistant properties.

Theoretical and experimental methods for multicomponent alloy weldment investigations have been limited in the past. The main theoretical problem was the absence of a more complex model for a multicomponent welded alloy system with dispersed phases that can describe the processes occurring in the weld joint with satisfactory accuracy. If it is accepted that a diffusion couple[8] may approximate a weld joint, it is then possible to perform a simulation of weldment temperature exposure using a model based on the Calphad approach[8] and complemented with the assumption that diffusion is the controlling process for the phase transformation rate,[4,9,10] the theory of multicomponent bulk diffusion,[6] thermodynamic evaluation of the driving force for phase transformations, and the assumption of local conditions of phase equilibrium. Such a theoretical model offers the possibility of obtaining highly complex theoretical results that agree very well with experimental diffusion couple observations.[11–15] The model is also implemented in the Dictra software package,[16] for example, and it enables a prediction to be made of the sequence of phase regions that are formed across the investigated weldment during the temperature exposure. Different creep strain rates are generally found in different regions of the weldment under external stress and this leads to the generation of increased mismatch stresses and premature failure.

The aims of the present work are: to present the results of weldment simulations for two weldments (CSN 15 128/P91 and SK3STC/P91), to compare the theoretical results with previous experiments,[17–19] and to suggest the relation between the simulated phase region sequence, weldment microstructure, and mechanical properties of the weld joint.

SUBJECT OF INVESTIGATION

The following materials and their weld joints were the focus of the present work (*see* Table 1 for detailed compositions): P91 steel alloyed with chromium and small amounts of molybdenum, vanadium, and nitrogen, CSN 15 128 low alloy Cr–Mo–V steel (according to Czech standard CSN 41 5128), and the consumable electrode material (Chromocord SK3STC). The progressive P91 steel represents creep resistant chromium steel for industrial applications.[20–22] The CSN 15 128 low alloy steel mentioned above is a frequently used steel because it gives a desirable combination of mechanical properties, resistance to corrosion, and cost.

DOI 10.1179/136217104225017161

Previous long term (up to 10 000 h) experiments[17–19] in the temperature range 500–700°C confirmed that the matrix of each investigated diffusion couple preserved the bcc_A2 (referred to as α below) structure with a time and distance dependent arrangement of carbides and/or carbonitrides. The development of the following dispersed phases was observed in the weldments: chromium rich carbides M_7C_3 and $M_{23}C_6$, special chromium poor carbide ($M_{23}C_6$), molybdenum rich carbide M_6C, molybdenum and vanadium rich carbide (M_2C), and vanadium rich carbonitride (MX, where X stands for both carbon and nitrogen).

SIMULATION MODEL

The following simplifying fundamental assumptions were used in the present model. The metastable phases or the stable phases with non-equilibrium compositions formed before post-weld heat exposure were excluded from the simulation. The width of the fusion zone was set equal to zero because the experimental fusion zone was also small (about 3×10^{-6} m). No heat affected zone generated during the weldment preparation was considered. The initial state of the weldment was approximated by two systems, each in equilibrium.

In the present simulations, the Calphad approach[8] was used for the solution of both local and global phase equilibrium problems in the steels investigated. Every investigated steel represents a multiclement system with several phases, i.e. the matrix phase and the dispersed phases (carbides and/or carbonitrides) included within it.

The Calphad approach permitted a solution based on constrained minimisation of the total Gibbs energy in a closed system at a given composition, temperature, and pressure. In short, the total Gibbs energy is calculated as a sum of molar phase Gibbs energies weighted by phase ratios. Using an appropriate thermodynamic model[23–28] the molar phase Gibbs energy can be evaluated as a function of temperature, pressure, phase composition, and 'thermodynamic parameters'. The parameters for selected phases and selected systems that represent the subsystems of the steels under examination can be found in the relevant literature. Numerically, this problem can be solved using available software packages (*see* Refs. 29–33 etc.). The following elements were considered for thermodynamic description of the materials examined: iron, chromium, molybdenum, vanadium, carbon, and nitrogen (cf. steel composition in Table 1). The Gibbs energy of the phases existing in this six element system was described using thermodynamic parameters from the STEEL12.TDB database.[34] This database contains data for the following subsystems: Fe–Cr–C, Fe–Mo–C, Fe–V–C, Fe–N–C, Fe–Cr–N, Fe–C–N, Cr–V–C, Cr–Mo–N, Mo–V–C, and Cr–Fe–V, and some data for higher subsystems, namely, Fe–Cr–Mo–C, Fe–Cr–V–C, Cr–V–Mo–C, and Cr–Fe–Mo–V–C. The phases were described using a regular solution model for phases with several components and sublattices:[23] α phase as the magnetic bcc_A2 phase with two sublattices $(Fe,Cr,Mo,V)_1(C,N,Va)_3$, where Va denotes vacancies; $M_{23}C_6$ as the stoichiometric phase with three sublattices $(Cr,Fe,V)_{20}(Cr,Fe,Mo,V)_3C_6$; M_7C_3 carbide as the stoichiometric phase with two sublattices $(Cr,Fe,Mo,V)_7C_3$; M_6C using a four sublattice description $Fe_2Mo_2(Cr,Fe,Mo,V)_2C$; and vanadium rich carbide M_2C and vanadium rich carbonitride MX were modelled as a non-stoichiometric phase $(Fe,Cr,Mo,V)_1(C,N,Va)_1$ using the parameters for the fcc_A1 phase.[35] This description was used to evaluate all the equilibrium quantities or functions presented (equilibrium composition, chemical potential, activity, etc.).

For a dissimilar weldment, a gradient of chemical potential can be observed and the diffusion[4] of the species proceeds at elevated temperatures. The changes in the chemical potentials of the species form the thermodynamic driving force for phase transformations, phase precipitation, growth, and/or phase dissolution. In the present paper the Dictra[16] program (including the ThermoCalc routines[29]) was used for the simulation of post-weld heat exposure. This model considers element mobilities[36] for diffusion matrix evaluation. The same selection of the species as for the thermodynamic description was considered for the kinetic description. The major interstitially diffusing species are carbon and nitrogen but the diffusion of the other substitutional species (iron, chromium, molybdenum, and vanadium) was also taken into account. The weldments were simulated as one-dimensional diffusion couples. Steel kinetics was approximated using the kinetic parameters for carbon and nitrogen mobility evaluations in bcc_A2 phase based on Fe–Cr–C and Fe–Cr–N[37,38] subsystems. The trace[39,40] diffusions of substitutional elements in iron were also included. The carbide and carbonitride phases were treated as non-diffusing spheroid phases suspended in the matrix. A local equilibrium between the matrix and the carbide/carbonitride phases was assumed in each part of the diffusion couple.

SIMULATION RESULTS

The simulation method permitted the prediction of any type of phase diagram cross-section for all the alloys investigated. The phase diagram cross-sections presented in Fig. 1*a* and *b* for P91 and CSN 15 128 respectively show equilibrium phases. The activities of the elements were also calculated for the alloys investigated. The carbon activity in the steels investigated is shown in Fig. 2.

The simulation using the Dictra program offers the time and distance dependence (profiles) for many parameters (molar phase ratio, overall concentration, both matrix and carbide element concentrations, activity, chemical potential, etc.). With respect to experimental work, the phase profiles and overall element concentration profiles are of greatest interest. Attention can sometimes also be focused on the element composition profile of the individual phases.

A simultaneous plot of the phase profiles is most appropriate to distinguish the phase regions across the weldment, the loading of the phases in the regions, and the width of the regions. The simulation results for two selected weldments are shown in Fig. 3. Generally, the sequence of the phase regions observed in the couple is time independent, the rate of the region interface motion increases non-linearly with distance from the initial weld interface, and the region width increases approximately with the square root of the time. The phase region sequences for simulated weldment combinations are summarised in Table 2. These sequences enabled the carbide reactions in progress in the weldments at given temperatures to be illustrated.

Table 1 Chemical composition of steels investigated, wt-%

Steel	C	Si	Mn	P	S	Cr	Mo	Ni	N	Nb	V
P91	0·10	0·43	0·40	0·015	0·006	8·50	0·88	0·10	0·045	0·018	0·23
CSN 15 128	0·13	0·31	0·60	0·012	0·022	0·58	0·47	0·07	…	…	0·25
SK3STC	0·12	0·07	0·80	0·008	0·011	2·73	0·96	0·02	…	0·013	0·01

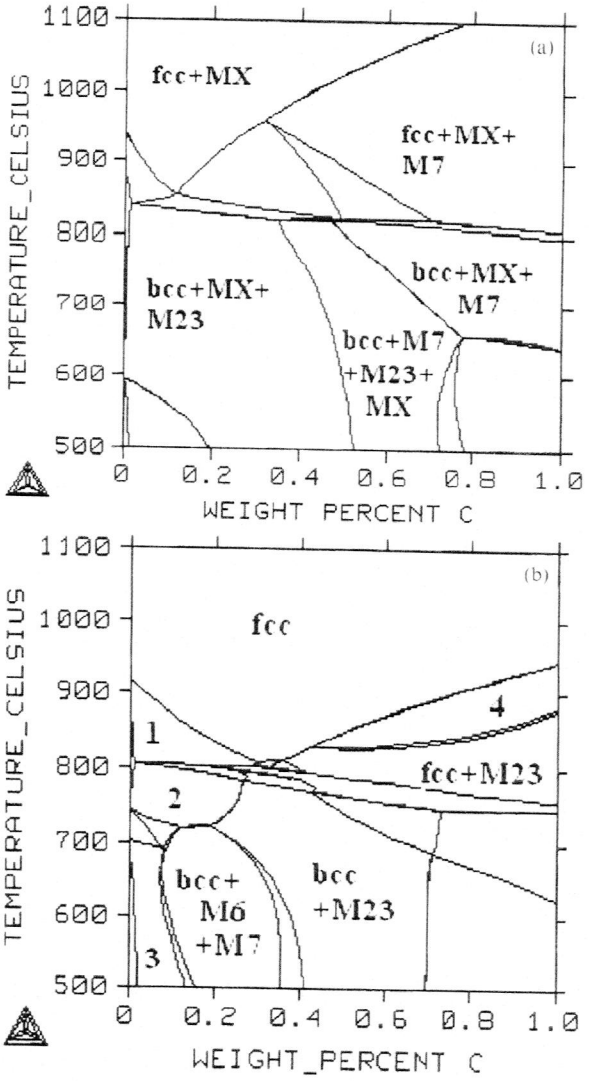

1 Phase diagram cross-sections for *a* steel P91 and *b* steel CSN 15 128 (1 bcc+fcc; 2 bcc+M_7C_3; 3 bcc+$M_{23}C_6$+M_6C; 4 fcc+M_7C_3)

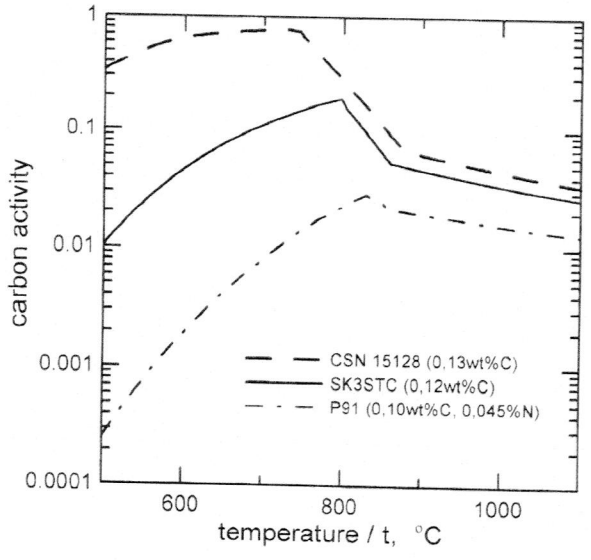

2 Variation of carbon activity of steels with temperature

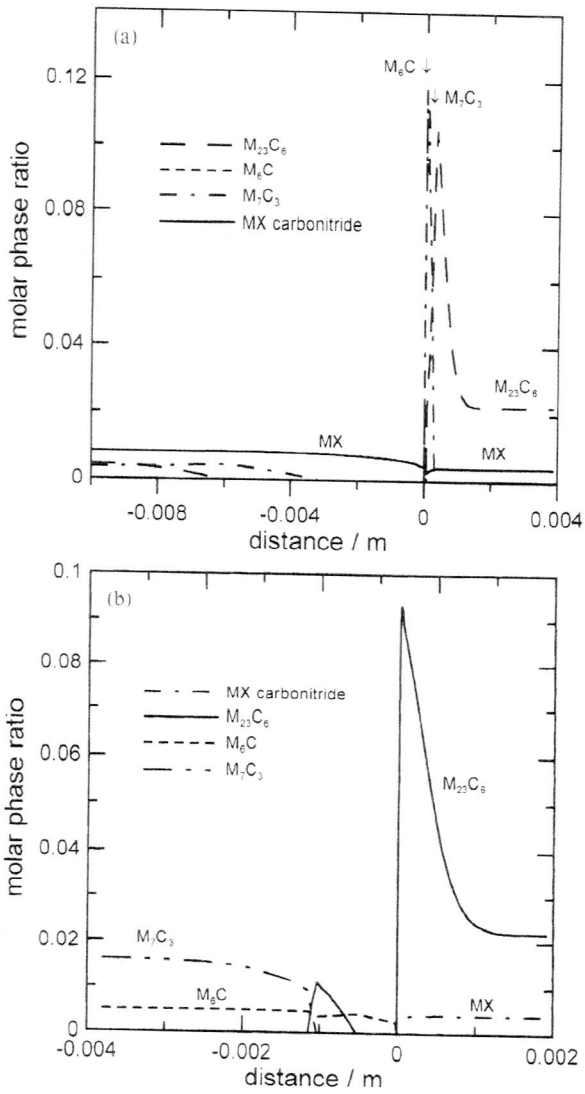

3 Simulated phase profiles for *a* CSN 15 128/P91 and *b* SK3STC/P91 weldments after 5000 h at 625 C

The simulation also permitted the calculation of the time and distance dependence for the composition of the dispersed phases. The carbonitride and $M_{23}C_6$ carbide composition profiles for the CSN 15 128/P91 weldment after post-weld heat treatment are shown in Fig. 4*a* and *b* respectively.

The overall concentration profiles can also be obtained from the simulation and they can be readily compared with experimental measurements.[17–19] Two experimental and simulated overall carbon concentration profiles are shown in Fig. 5, where numerous experimental observations[17] are represented by fitted experimental curves.

DISCUSSION

The Calphad method enables the phase diagrams of steels to be calculated with high reliability and with relatively little experimental work. The phase diagram predictions in Fig. 1 obtained using the STEEL12 thermodynamic database[34] can be performed for other technical steels also. The phase diagram predictions may differ if a different thermodynamic database is used (for example SSOL[29]), especially in low temperature ranges. However, it is the present authors' opinion that the STEEL12 thermodynamic database used yields more accurate results because it is

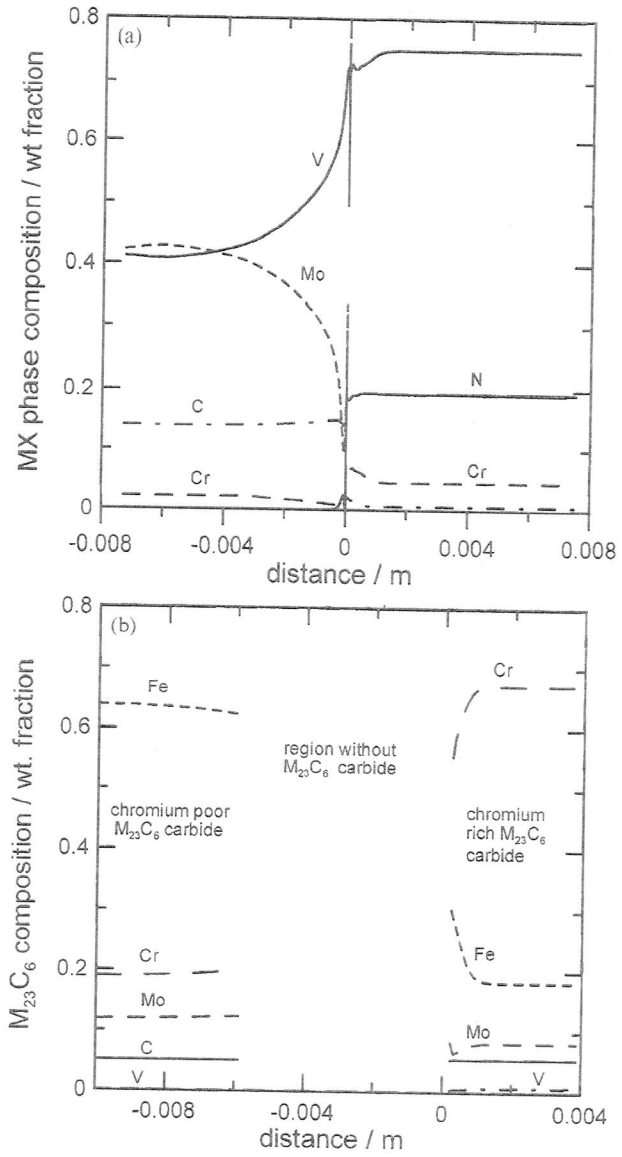

4 Simulated chemical composition of *a* MX carbonitride and *b* $M_{23}C_6$ carbide as function of distance from interface (CSN 15 128/P91 weldments, 625°C/5000 h)

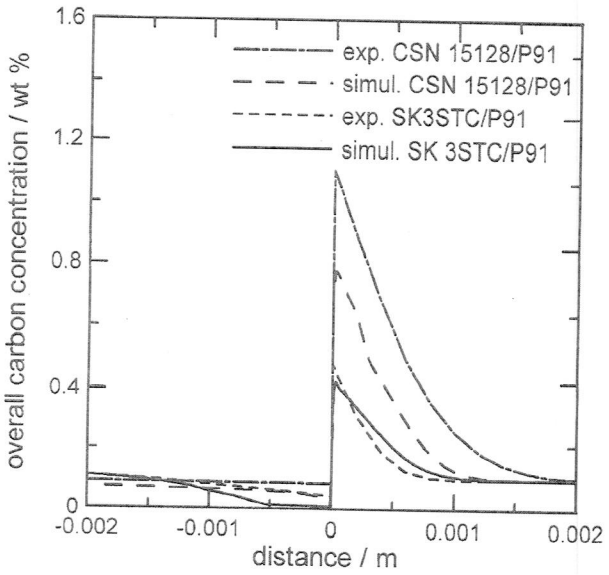

5 Simulated and experimental overall concentration profiles after 5000 h at 625°C

optimised for lower temperatures. The same emphasis is placed on the consistency of the DIF12 kinetic database[41] at low temperatures.

The high temperature microstructure stability or instability of dissimilar weldments may be considered in different ways. In the first approximation, the element activity in steels can be used as a determinative value for weld joint stability. The carbon and/or nitrogen activity is of high importance (*see* Fig. 2). From this simple viewpoint, the SK3STC steel represents a convenient electrode material for the fabrication of the CSN 15 128/SK3STC/P91 complex weld joint because the curve of carbon activity for the consumable lies between the curves for the joined materials. However, this approach is not sufficient for a long term stability/instability judgement.

In the second approximation, the simulated phase and element profiles can be used to obtain an estimation of the lifetime of weld joints and consequently to obtain the remaining lifetime for technological installations. The phase region sequence (*see* Table 2) and phase profile (*see* Fig. 3) can assist in determining the weakest point inside the

Table 2 Weldment combinations, annealing conditions, and simulated phase region sequences

Weldment combinations	Temperature, °C	Phase region sequence (predominant carbide/carbonitride in bold type)
CSN 15 128/P91	500 – 561	$(\alpha+M7+\mathbf{MX})<(\alpha+M23+M7+\mathbf{MX})<(\alpha+M7+\mathbf{MX})<(\alpha+\mathbf{MX})\|(\alpha+\mathbf{M6}+MX)>(\alpha+M6+\mathbf{M7}+MX)>(\alpha+\mathbf{M23}+M6+M7+MX)>(\alpha+\mathbf{M23}+M6+MX)$
CSN 15 128/P91	561 – 577	$(\alpha+M7+\mathbf{MX})<(\alpha+M23+M7+\mathbf{MX})<(\alpha+M7+\mathbf{MX})<(\alpha+\mathbf{MX})\|(\alpha+\mathbf{M6}+MX)>(\alpha+M6+\mathbf{M7}+MX)>(\alpha+\mathbf{M23}+M6+M7+MX)>(\alpha+\mathbf{M23}+M7+MX)>(\alpha+\mathbf{M23}+MX)$
CSN 15 128/P91	577 – 655	$(\alpha+M23+M7+\mathbf{MX})<(\alpha+M7+\mathbf{MX})<(\alpha+\mathbf{MX})\|(\alpha+\mathbf{M6}+MX)>(\alpha+M6+\mathbf{M7}+MX)>(\alpha+\mathbf{M23}+M6+M7+MX)>(\alpha+\mathbf{M23}+M7+MX)>(\alpha+\mathbf{M23}+MX)$
CSN 15 128/P91	655 – 700	$(\alpha+\mathbf{M23}+MX)<(\alpha+\mathbf{MX})\|(\alpha+\mathbf{M6}+MX)>(\alpha+M6+\mathbf{M7}+MX)>(\alpha+\mathbf{M23}+M6+M7+MX)>(\alpha+\mathbf{M23}+M7+MX)>(\alpha+\mathbf{M23}+MX)$
SK3STC/P91	500 – 554	$(\alpha+\mathbf{M23}+M6)<(\alpha+\mathbf{M6})<(\alpha+\mathbf{M23}+M6)\|(\alpha+M6+\mathbf{M23}+MX)>(\alpha+\mathbf{M23}+MX+M6)>(\alpha+M7+MX+\mathbf{M23}+M6)>(\alpha+MX+\mathbf{M23}+M6)$
SK3STC/P91	554 – 556	$(\alpha+\mathbf{M7}+M6+M23)<(\alpha+\mathbf{M23}+M6)<(\alpha+\mathbf{M6})<(\alpha+\mathbf{M23}+M6)\|(\alpha+M6+\mathbf{M23}+MX)>(\alpha+\mathbf{M23}+MX+M6)>(\alpha+M7+MX+\mathbf{M23}+M6)>(\alpha+MX+\mathbf{M23}+M6)$
SK3STC/P91	556 – 561	$(\alpha+\mathbf{M7}+M6)<(\alpha+M7+M6+\mathbf{M23})<(\alpha+\mathbf{M23}+M6)<(\alpha+\mathbf{M6})<(\alpha+\mathbf{M23}+M6)\|(\alpha+M6+\mathbf{M23}+MX)>(\alpha+\mathbf{M23}+MX+M6)>(\alpha+M7+MX+\mathbf{M23}+M6)>(\alpha+MX+\mathbf{M23}+M6)$
SK3STC/P91	561 – 700	$(\alpha+\mathbf{M7}+M6)<(\alpha+M7+M6+\mathbf{M23})<(\alpha+\mathbf{M23}+M6)<(\alpha+\mathbf{M6})<(\alpha+\mathbf{M23}+M6)\|(\alpha+M6+\mathbf{M23}+MX)>(\alpha+\mathbf{M23}+MX)>(\alpha+M7+MX+\mathbf{M23})>(\alpha+MX+\mathbf{M23})$

*Phase abbreviations used: α bcc_A2; M7 M_7C_3; M23 $M_{23}C_6$; M6 M_6C; MX carbonitride. Symbols '<' and '>' indicate that interface is moving to left and right with time respectively; symbol '|' indicates negligible movement.

weldment because the mechanical properties of the region can be estimated from the phase microstructure.[42]

The simulation result corresponds with experimental observations[17–19] and any possible discrepancies observed can be readily explained by the limitations of experimental technique, preweld heat treatment, or simulation model limitations. The carbide types found experimentally in steel weldments correspond well with the diffusion couple simulation (*see* Fig. 3). All the above results confirm the stability of MX carbides during post-weld temperature exposure across the whole CSN 15 128/P91 weldment (Fig. 3*a*), $M_{23}C_6$ carbide nucleation and coarsening in the P91steel, the formation of a carbon depleted zone close to the initial weld interface (*see* Fig. 5), etc. The simulation also shows the same predominant M_6C carbide that formed a narrow band of coarse carbides on the experimental CSN 15 128/P91 weld interface[17] (*see* Fig. 3*a* and Table 2). Further, the simulations confirmed the existence of the phase regions $\alpha+MX$ (CSN 15 128/P91) and $\alpha+M_6C$ (SK3STC/P91), which were found experimentally inside the carbon depleted zone (*see* the temperature range including 625°C in Table 2).

The experimental and simulated carbide/carbonitride compositions are also in good agreement. For example, the simulation confirmed the variation in the $M_{23}C_6$ carbide composition in the experimental CSN 15 128/P91 weldment[17] (*see* Fig. 4*b*). The simulations predict carbon rich and nitrogen rich carbonitrides. The simulated chemical composition of MX carbonitride (Fig. 4*a*) reflects the high molybdenum and vanadium content of the experimental alloy.

For comparison, the carbide metal composition (i.e. individual metal contents per total amount of metals in wt-%) 35Mo–55V–7Cr was also observed[43] in similar 0·6Cr–0·4Mo–0·3V–0·15C steel (*see* Table 1 for CSN 15 128 alloy composition) and high molybdenum content (up to 50 wt-%) was found in MC carbide in a similar instance.[44] These experimental observations show that MX carbonitride thermodynamic modelling using thermodynamic parameters of the fcc_A1 phase[35] gives a fairly reasonable approximation. Another experimental observation in CSN 15 128 steel[44] shows a majority of MC, M_7C_3, and $M_{23}C_6$ carbides and a minority of M_2C carbide at temperatures close to 625°C. Therefore, it was decided to exclude M_2C carbide from the present simulations.

Examples of the experimental and simulated bulk carbon profiles are shown in Fig. 5. The extreme experimental values (peak maximum/minimum) agree, within the limits of accuracy of the experimental measurement, with the simulated values. In Fig. 5, the lower simulated maximum carbon concentration in the CSN 15 128/P91 weldment carburised zone can be seen. This can be readily explained by grain boundary diffusion, which is not included in the simulation model.

It can be stated that both weldment combinations (CSN 15 128/P91 and SK3STC/P91) represent fairly sound joints under the conditions investigated. However, there is a risk of decarburising the bcc_A2 zone formed during long term exposure. This risk is reduced by carbide and/or carbonitride particles. It was found by simulation and also by experiment that the decarburised CSN 15 128/P91 zone contains the MX carbonitride and the decarburised SK3STC/P91 zone contains the M_6C carbide. The $M_{23}C_6$ carbide predominates in the carburised zones of both weldments. The CSN 15 128/P91 (*see* Table 2) simulated phase region sequence includes a central $(\alpha+MX)|(\alpha+M6+MX)$ subsequence (where M6 represents M_6C) with a high quantity of M_6C carbide. This reflects experimental results.[17]

Other phases (Laves, M_5C, V_4C_3, PI phase) were also considered in weldment simulation. One of these, the Laves phase, represents a great risk to the soundness of the weld. This phase has not been mentioned because it is not stable under the simulated conditions but a small concentration shift or addition of another Laves phase stabilising element (e.g. manganese) may cause Laves phase precipitation in the P91 steel or in the decarburised zone. The simulation confirms that the Laves phase occurs at temperatures below 600°C and at lower carbon concentrations (approximately <0·01 wt-%).

CONCLUSION

The above approach and the simulation results enabled an improved understanding to be reached of the microstructural processes and carbide and/or carbonitride phase transformations occurring in the diffusion zone of the investigated weldments. It can be generally stated that the method applied yields results that reflect the weldment phase structure fairly accurately.

A good agreement was found in the sequence of the carbide and/or carbonitride phase regions.

The kinetic simulations performed provided information that can be used for failure risk prediction for weld joints. The simulated phase profiles for the vanadium rich MX carbonitride and the M_6C carbide showed their microstructure stabilising effect in the investigated weldments. Special attention must be paid to the concentration balance, which may be responsible for the Laves phase precipitation in weldments that include the P91 steel.

The simulation results save time and expense in the evaluation of long term microstructural stability of the weldments examined. The profiles presented can serve in the prediction of microstructure development and estimation of the mechanical stability of the weldments under external stress during long term service.

ACKNOWLEDGEMENTS

The support of the Grant Agency of the Czech Republic (no. 106/00/0855) in funding the present work is gratefully acknowledged. The calculations were performed with the aid of the ThermoCalc and Dictra programs. Sincere thanks are extended to Professor J. Vřestá for thermodynamics and kinetics calculations.

REFERENCES

1. V. PILOUS and K. STRANSKY: in 'Structural stability of deposits and welded joints in power engineering', 97–159; 1998, Cambridge, UK, Cambridge Int. Science Publishers.
2. M. WITWER, H. CERJAK and B. BUCHMAYR: Proc. Int. Conf. on 'High temperature materials for power engineering', Liege, Belgium, September 1990, Université de Liège, 751–760.
3. B. MILLION, K. BACILEK, J. KUCERA, P. MICHALICKA, A. REK and K. STRANSKÝ: *Z. Metallkd.*, 1995, **86**, 706–712.
4. J. S. KIRKALDY and D. J. YOUNG: 'Diffusion in the Condensed State'; 1985, London, The Institute of Metals.
5. R. FORET, K. STRANSKÝ, J. KRUMPOS, B. MILLION and V. PILOUS: Proc. Int. Conf. on 'Integrity of high-temperature welds', 135–142; 1998, Suffolk, UK, The Institution of Mechanical Engineers/The Ipswich Book Company.
6. J. O. ANDERSSON, L. HÖGLUND, B. JÖNSSON and J. ÅGREN: in 'Fundamentals and applications of ternary diffusion', (ed. G. R. Purdy), 153–163; 1990, New York, Pergamon Press.
7. D. A. PORTER and K. E. EASTERLING: 'Phase transformations in metals and alloys'; 1986, Thetford, Norfolk, UK, The Thetford Press Ltd.
8. N. SAUNDERS and A. P. MIODOVNIK: 'CALPHAD (calculation of phase diagram) – a comprehensive guide', Pergamon Materials Series, Vol. 1, 299–458; 1998, Amsterdam, Elsevier Science.
9. A. ENGSTRÖM, L. HÖGLUND and J. ÅGREN: *Metall. Mater. Trans. A*, 1994, **25A**, 1127–1134.
10. A. BORGENSTAM, A. ENGSTRÖM, L. HÖGLUND and J. ÅGREN: *J. Phase Equilibria*, 2000, **21**, 269–280.
11. T. HELANDER and J. ÅGREN: *Metall. Mater. Trans. A*, 1997, **28A**, 303–308.

12. T. HELANDER, J. ÅGREN and J. O. NILSSON: *ISIJ Int.*, 1997, **37**, 1139–1145.
13. E. KOZESCHNIK, P. PÖLT, S. BRETT and B. BUCHMAYR: *Sci. Technol. Weld. Joining*, 2002, **7**, 63–68.
14. E. KOZESCHNIK, P. WARBICHLER, I. LETOFSKY-PAPST, S. BRETT and B. BUCHMAYR: *Sci. Technol. Weld. Joining*, 2002, **7**, 69–76.
15. N. C. SEKHAR and R. C. REED: *Sci. Technol. Weld. Joining*, 2002, **7**, 77–87.
16. 'User's guide: DICTRA (v. 20)', Division of Physical Metallurgy, Department of Materials Science and Engineering, Royal Institute of Technology, Stockholm, 1998.
17. R. FORET, B. MILLION, M. SVOBODA and K. STRÁNSKÝ: *Sci. Technol. Weld. Joining*, 2001, **6**, 405–411.
18. B. MILLION, R. FORET, A. REK and K. STRÁNSKÝ: *Kovové Mater.*, 1999, **37**, (5), 314–323.
19. M. SVOBODA and I. PODSTRANSKA: Proc. Int. Conf. on 'Corrosion-resistant steels and alloys at the turn of century', Řeka, Czech Republic, October 1999, Technical University of Ostrava, 132–135.
20. B. IRVING: *Weld. J.*, 2001, **80**, 40–44.
21. A. ORLOVÁ, J. BURŠÍK, K. KUCHAŘOVÁ and V. SKLENICKA: *Mater. Sci. Eng. A*, 1998, **A245**, (1), 39–48.
22. J. ČADEK, V. ŠUSTEK and M. PAHUTOVÁ: *Mater. Sci. Eng. A*, 1997, **A225**, 22–28.
23. B. SUNDMAN and J. ÅGREN: *J. Phys. Chem. Solids*, 1981, **42**, 297–301.
24. O. REDLICH and A. T. KISTER: *Ind. Eng. Chem.*, 1948, **40**, 345–352.
25. M. HILLERT and L. I. STAFFANSON: *Acta Chem. Scand.*, 1970, **24**, 3618–3656.
26. M. HILLERT and M. JARL: *Calphad*, 1978, **2**, 227–232.
27. G. INDEN: *Z. Metallkd.*, 1975, **66**, 577–584.
28. G. INDEN: *Physica B*, 1981, **103B**, 82–90.
29. 'User's guide: ThermoCalc (v. M)', Division of Computational Thermodynamics, Department of Materials Science and Engineering, Royal Institute of Technology, Stockholm, 1997.
30. 'User's guide: PANDAT software for multicomponent phase diagram calculation', CompuTherm LLC, Madison, WI, USA, 2000.
31. J. SOPOUŠEK, A. KROUPA, R. DOJIVA and J. VŘEŠŤÁL: *Calphad*, 1993, **17**, 229–235.
32. 'Web sites in inorganic chemical thermodynamics, FACT', Internet http://www.crct.polymtl.ca/fact/websites.htm.
33. 'Thermodynamic database: MALT2', Internet http://www.kagaku.com/malt/emalt2.html.
34. A. KROUPA, J. HAVRÁNKOVÁ, M. COUFALOVÁ, M. SVOBODA and J. VŘEŠŤÁL: *J. Phase Equilibria*, 2001, **22**, 312–323.
35. B. J. LEE and D. N. LEE: *J. Phase Equilibria*, 1992, **13**, 349–363.
36. J. O. ANDERSON and J. ÅGREN: *J. Appl. Phys.*, 1992, **72**, 1350–1355.
37. B. JÖNSSON: *Z. Metallkd.*, 1994, **85**, 497–501.
38. V. JAN, J. SOPOUŠEK and R. FORET: Proc. Conf. 'Metal 2002', Hradec nad Morvicí, Czech Republic, May 2002, TANGER, S. R. O., 1–7.
39. J. KUČERA and K. STRÁNSKÝ: *Mater. Sci. Eng.*, 1982, **52**, 1–38.
40. H. OIKAWA: *Technol. Rep. Töhoku Univ.*, 1983, 7–77.
41. V. JAN and J. SOPOUŠEK: Proc. Int. Conf. on: 'Thermodynamics of alloys' (TOFA 2002), Rome, September 2002, Universitá di Roma 'La Sapienza', 55.
42. R. RAJEEV, I. SAMAJDAR, R. RAMAN, C. S. HARENDRANATH and G. B. KALE: *Mater. Sci. Technol.*, 2001, **17**, 1005–1011.
43. P. UNUCKA, A. KROUPA, R. FORET and M. SVOBODA: to be published in *J. Phase Equilibria*.
44. V. FOLDYNA: 'Creep of low alloyed and modified chromium steels', DSc thesis, Institute of Physics of Materials, Academy of Sciences of Czech Republic, Brno, Czech Republic, 1988.